Supporting information

Recyclable superhydrophobic, anti-moisture activated carbon pellets for air and water purification

Xuan Jiao,† Meiting Li,† Zhen Cheng,† Xinquan Yu,† Shu Yang,‡ and Youfa Zhang,†*

† Jiangsu Key Laboratory of Advanced Metallic Materials, School of Materials Science and Engineering, Southeast University, Southeast Road 2nd, Nanjing 211189, P. R. China.

‡ Department of Materials Science and Engineering, University of Pennsylvania, 3231 Walnut Street, Philadelphia, PA 19104, USA

Corresponding Author

*E-mail: yfzhang@seu.edu.cn

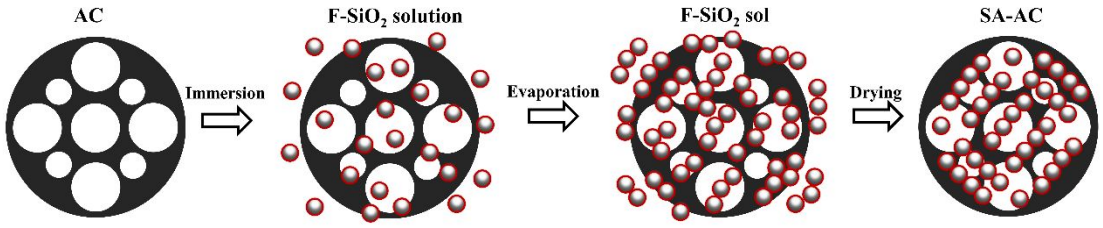

Figure S1. Schematic illustrations on the process of the synthesis for superhydrophobic activated carbons pellets. The ratio of mass to volume for activated carbon pellets and superhydrophobic silica sol was 1:2, and the treatment was conducted at the temperature of 50 ℃ for 4 h.

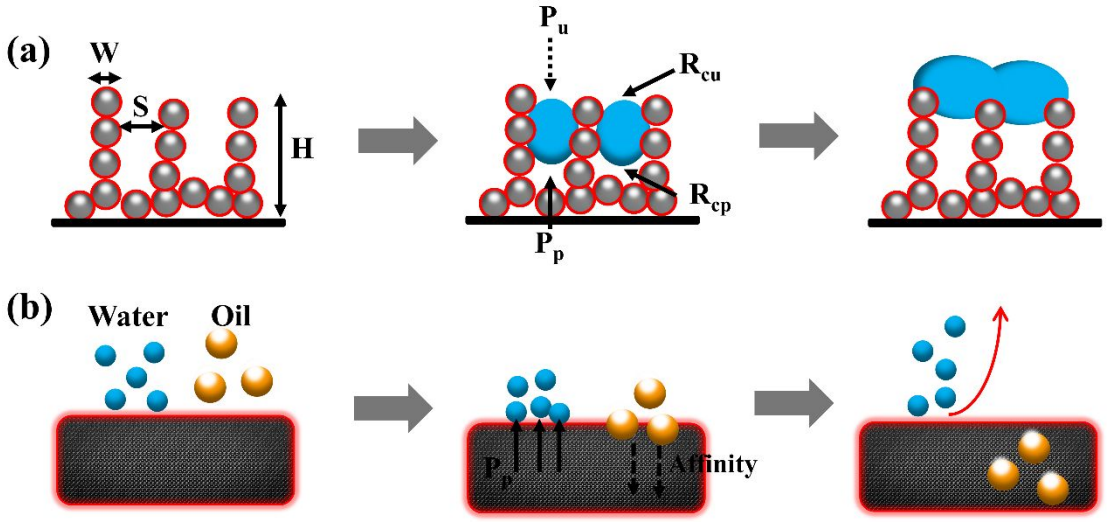

Figure S2. (a) The schematic diagram whole process and air pressure effect on the surface. (b) The demonstration and mechanism analysis of water and oil droplets during the adsorption process.

Due to the self-assembly of superhydrophobic nanoparticles, the micro/sub-micropores are universally distributed on the surface of SA-AC with height (H), width (W), and sub-micro/micropore size (S). The schematic diagram is presented in Figure S2, showing the whole process and air pressure effect on the surface. As the microdrops growing, the pressure of pocket air (Pp) increases gradually, as a result of the internal compression and capillary effect. Furthermore, the coalescence of microdrops leads to

the dramatic increase on curvature radius of the upside liquid-gas interface (Rcu), accordingly, causing the decrease on the pressure of the upside air (Pu) based on the Laplace's law. And the difference between Pu and Pp induces the repellence of water microdrops, manifesting good effect for anti-moisture. For the adsorption of oil and MB, the water drops are pushed away by the increasing Pp, thus resulting in rapid penetration of oil and MB. Meanwhile, SA-AC holds strong affinity to them, enhancing the adsorption capacity at the condition of water repellence. But the molecule of oil is relatively large and equipped with low surface tension, it's a little difficult for SA-AC to release oil molecules for recyclability.

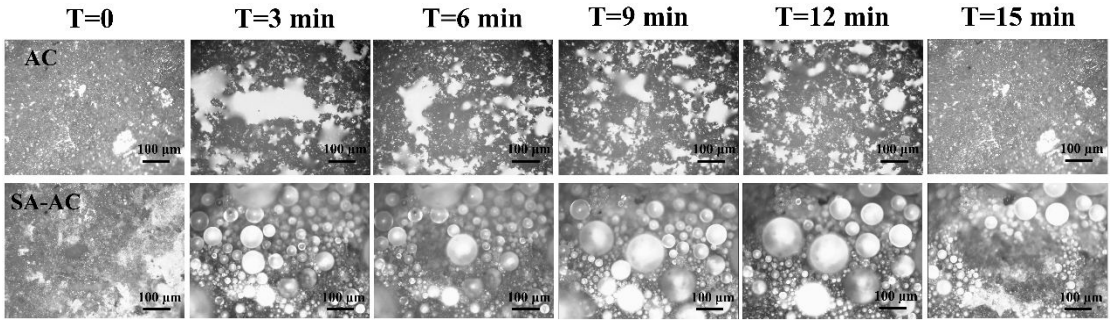

Figure S3. Condensation images of the surface of AC and SA-AC pellets.

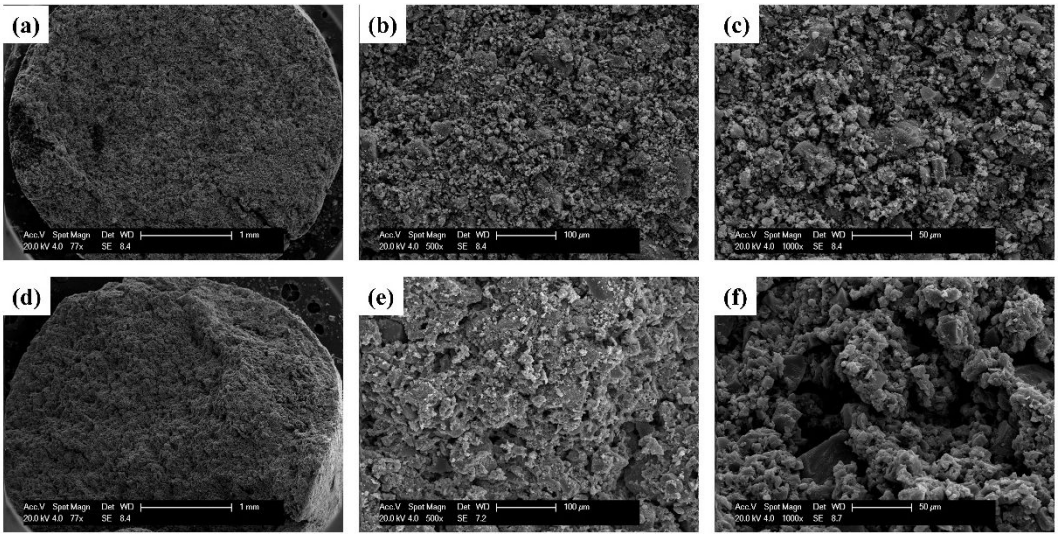

Figure S4. SEM images with different magnifications of initial AC pellets (a)~(c) and SA-AC (d)~(f) pellets.

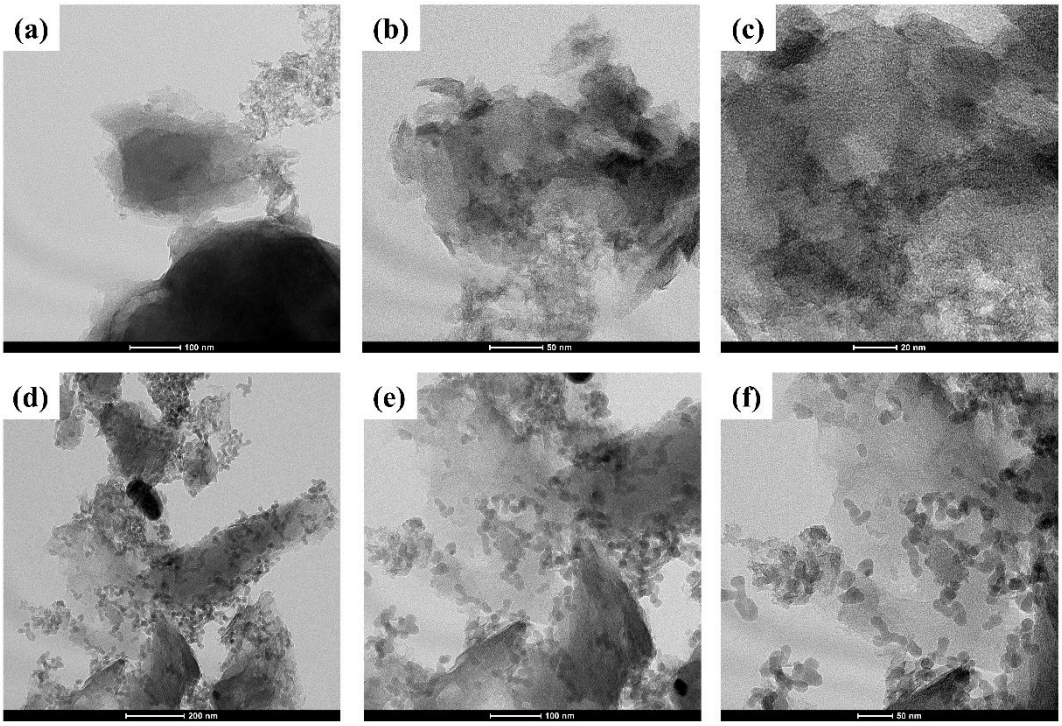

Figure S5. TEM images with different magnifications of initial AC pellets (a)~(c) and SA-AC (d)~(f) pellets.

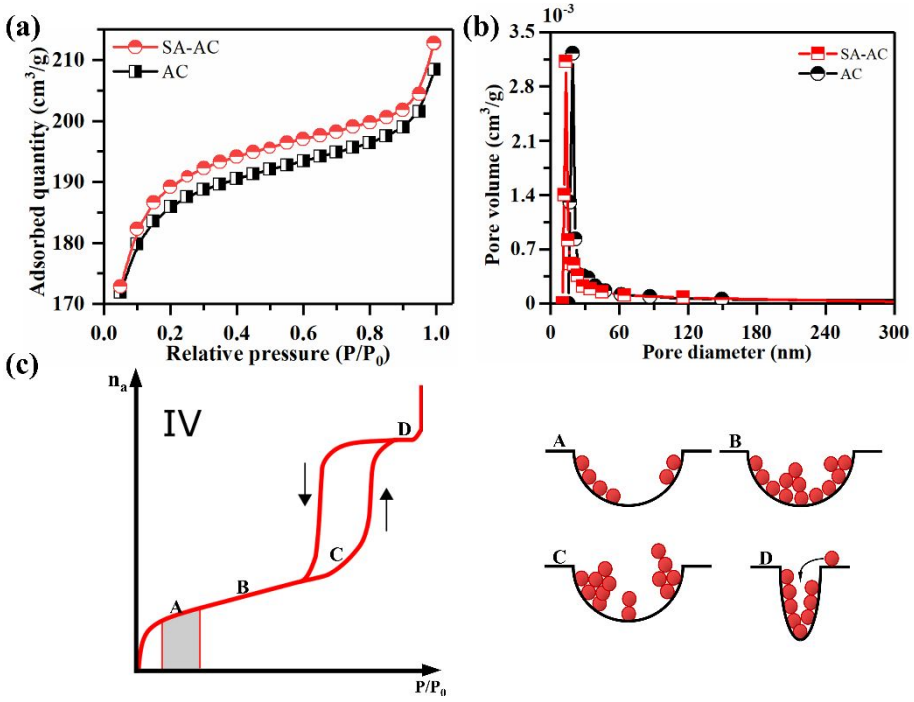

Figure S6. (a) Adsorption isotherms on nitrogen of SA-AC and AC at 77 K. (b) The pore size distributions of AC and SA-AC according to BJH (Barrett–Joiner–Halenda) method with desorption summary. (c) The adsorption isotherm of type IV on nitrogen of AC and SA-AC pellets at the temperature of 77 K according to Brunauer-Deming-Deming-Teller classification.

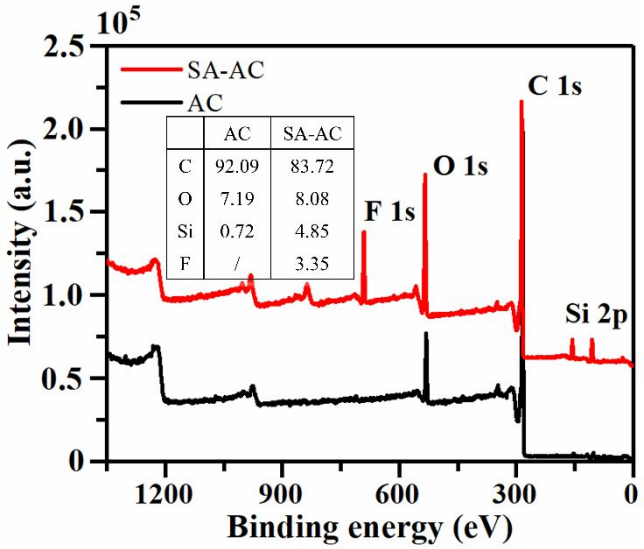

	AC	SA-AC
C	92.09	83.72
O	7.19	8.08
Si	0.72	4.85
F	/	3.35

Figure S7. Wide-scan XPS spectra on the surface elements of AC and SA-AC.

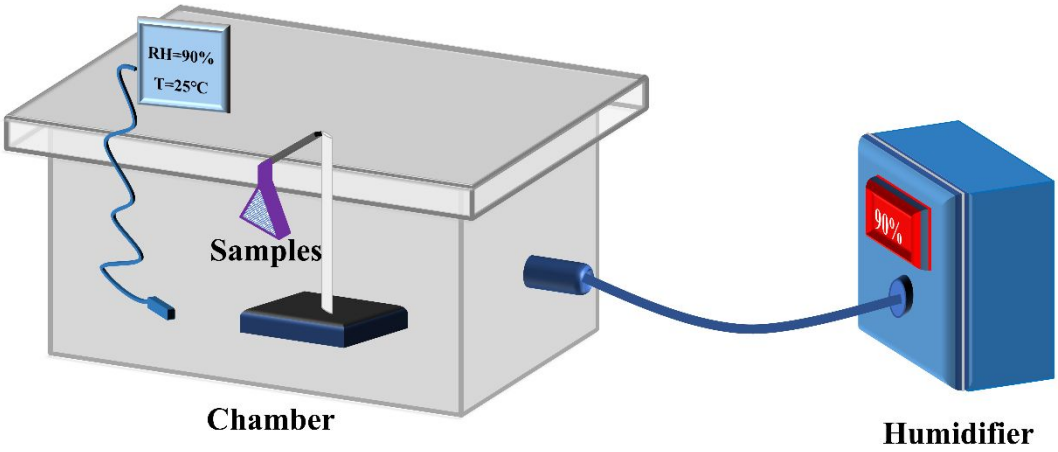

Figure S8. Schematic illustrations of the self-manufacture device of moisture adsorption test system on different AC pellets at ambient temperature.

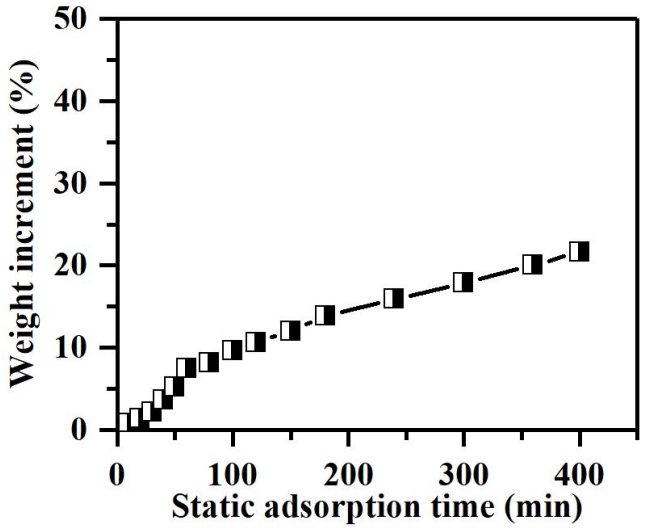

Figure S9. Moisture adsorption tests with RH of 90% at indoor temperature on superhydrophobic AC modified through chemical vapor deposition (CVD).

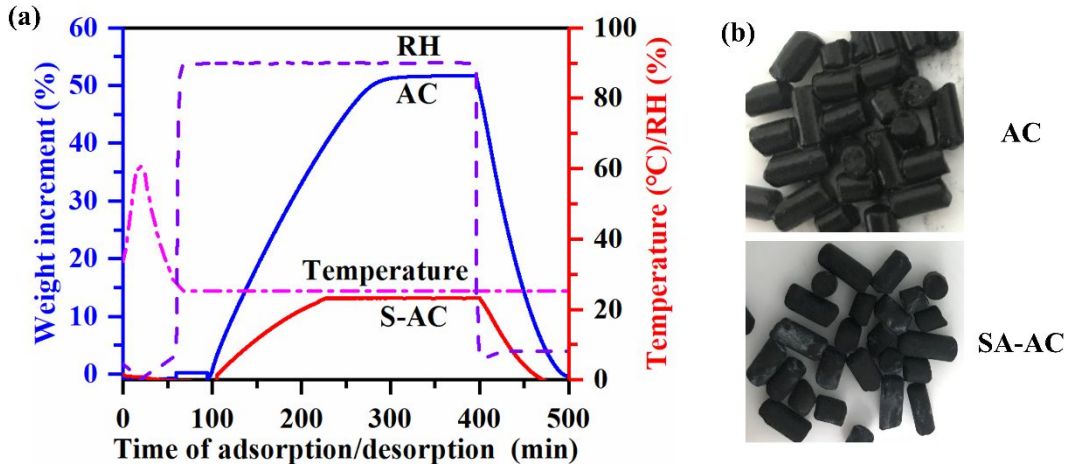

Figure S10. (a) The dynamic water adsorption tests at the indoor temperature under the condition of constant relative humidity of AC and SA-AC, conducted on the automatic vapor adsorption analyzer. (b) The optical images of AC and SA-AC pellets after the process of 400 min moisture adsorption.

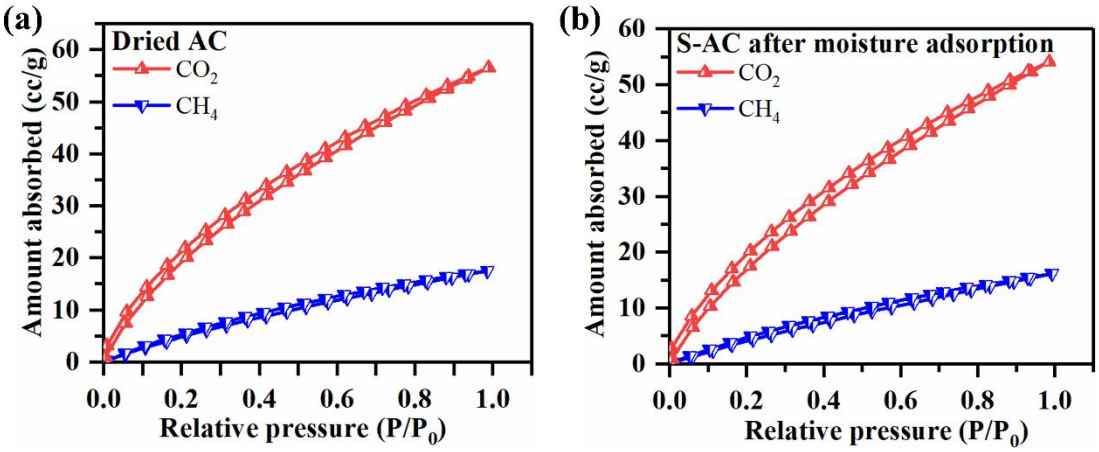

Figure S11. (a) The adsorption-desorption isotherms at the temperature of 323 K on different organic gases (CH_4 and CO_2) of dried AC pellets without modification. (b) The adsorption-desorption isotherms at the temperature of 298 K on different organic gases (CH_4 and CO_2) of SA-AC after static moisture adsorption with humidity of 90% for 90 min. The absence of the result on

AC due to the loss of adsorbed ability for gases after severe adsorption of moisture.

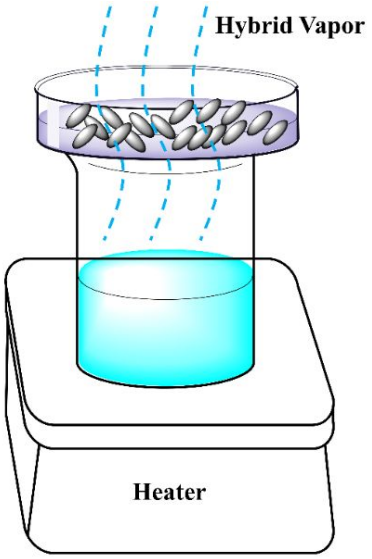

Figure S12. Schematic illustrations of the self-manufacture device for hybrid vapor adsorption tests on different AC pellets.

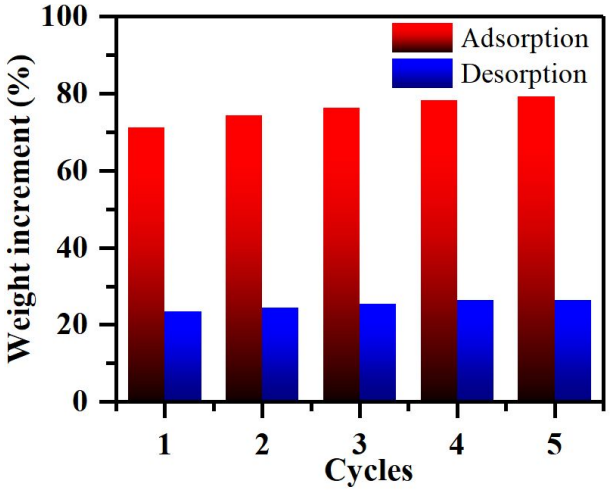

Figure S13. The recoverable tests on hybrid vapor adsorption and desorption of AC for 5 cycles.

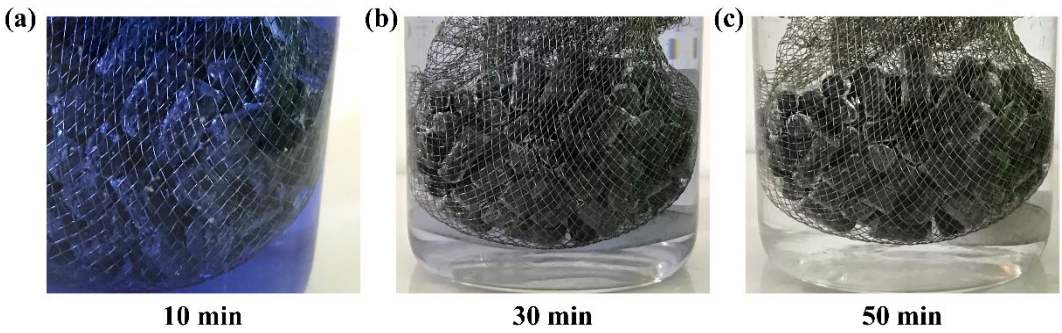

Figure S14. The magnified optical images of SA-AC pellets in MB aqueous solutions at the time of 10 min (a), 30 min (b) and 50 min (c).

Figure S15. The static contact angle of 5 μL oil on AC and SA-AC.

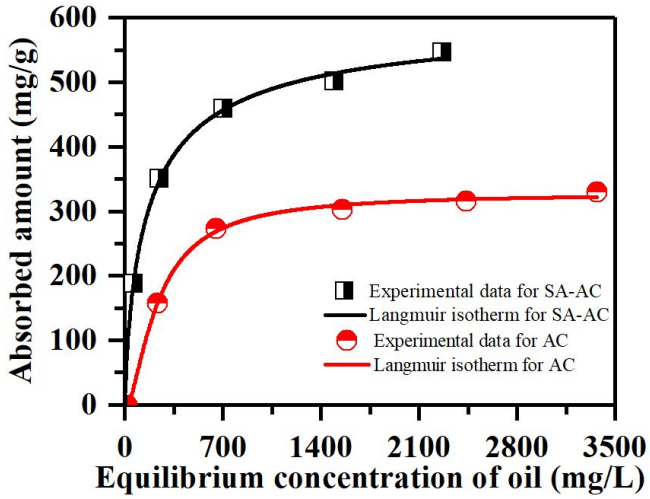

Figure S16. Langmuir model isotherm for oil removal at the temperature of 40 ℃ with varying initial concentration from 500 to 2500 mg·L^{-1} on AC and SA-AC pellets.